36th AIAA Plasmadynamics and Lasers Conference AIAA-2005-4774
6-9 June 2005, Toronto, Canada

Regularizing Shear Layer for Adaptive Optics Control Applications

Alice M. Nightingale[*], Stanislav Gordeyev[**], Eric J. Jumper[†], Bill Goodwine[‡] and John P. Siegenthaler[§]
University of Notre Dame, Notre Dame, IN, 46556

This paper uses a discrete-vortex code to examine a shear layer's response to forcing at its origin. The code and its thermodynamic overlay have been used in previous studies to predict the optically-aberrating characteristics of relatively-high-Mach-number, subsonic shear layers that can be classified as weakly compressible. The results reported in this study are again directed toward the shear layer's optical characteristics; however, the intent was to use forcing to create periodic aberrating fields, referred to as "regularized" shear-layer aberrations. The study shows that the use of single-frequency forcing produces a regularized shear layer for distances preceding the point where the unforced shear layer's natural frequency occurs. In the case of the forced shear layer, a greater thickness is produced closer to its point of origin until collapsing onto the unforced shear layer thickness past the point of regularization. The aberration periodicity is shown to have lower robustness toward the furthest downstream extent of regularization due to uncontrolled pairing. This region is made more regular by applying both fundamental and subharmonic forcing at the shear layer's origin; however, such subharmonic forcing is sensitive to the phasing of the fundamental to that of the subharmonic.

I. Introduction

When an otherwise planar optical wavefront is made to propagate through a relatively-high Mach number subsonic shear layer the wavefront becomes aberrated (see Fig. 1) adversely affecting its far-field intensity pattern. This degraded far-field intensity pattern is undesirable for use in optical systems. Since the early 1990s, the optical characteristics of free shear layers have been the subject of investigation. The cause of the optical aberrations in shear layers was found to be the large scale structures that naturally "roll up." More particularly, it was found that the radial pressure gradients (and the associated density deficit) required to support the curvature of the structure were the cause of a large part of the optical aberrations[1]. For a shear layer experimentally investigated in Ref. 2 with a Mach 0.8 high-speed side and a Mach 0.1 low-speed side, the aberrations approximately 0.5 m downstream from its point of origin are sufficient to reduce its far-field intensity by 98% of its otherwise unaberrated, diffraction-limited far-field intensity.

It has long been known that placing a conjugate waveform on the optical wavefront of a laser beam prior to its transmission through the aberrating medium in the case of an outgoing laser, for example, results in the emergence of a planar-wavefront beam as it leaves the medium (see Fig. 1). Systems that sense the aberration and construct and apply the proper conjugate waveform at regular time intervals are termed *adaptive-optic (AO) systems*[3].

A traditional AO system operates in consecutive steps; the first step is to sense the aberration for which a conjugate must be constructed. Since optics is linear, this aberration can be determined by measuring the aberrated wavefront from a source propagating through the aberrating flow from either direction. For projecting systems, determining the aberration (or the remaining residual aberration after a correction has been made) at any given instant is done by sensing the aberration from an incoming optical signal. The wavefront aberration is measured using a *WaveFront Sensor (WFS)*. Once the wavefront's figure is measured a *Conjugate Constructor (CC)*, sometimes referred to as a "*reconstructor*," determines the distorted pattern that must be sent to a *deformable mirror (DM)*. Although the speed of this CC is important (c.f., below), in general the CC is typically much faster than the WFS and, *at present*, does not

[*] Graduate Research Assistant, Department of Aerospace and Mech. Eng, AIAA Student Member.
[**] Assistant Research Professor, Department of Aerospace and Mech. Eng., Member AIAA.
[†] Professor, Department of Aerospace and Mech. Eng., Fellow AIAA
[‡] Associate Professor, Department of Aerospace and Mech. Eng.
[§] Graduate Research Assistant, Department of Aerospace and Mech. Eng, AIAA Student Member.

form the bandwidth-limiting step. This conjugate (or some portion of it, see below) is then sent to a DM, whose electro-mechanical character, including its source of excitation (i.e., amplifiers), limits the rate at which it can respond to signals adjusting its figure. The conjugate wavefront is placed on the laser prior to its propagation through the aberrating turbulence by first reflecting it off the DM (see Fig. 1, right).

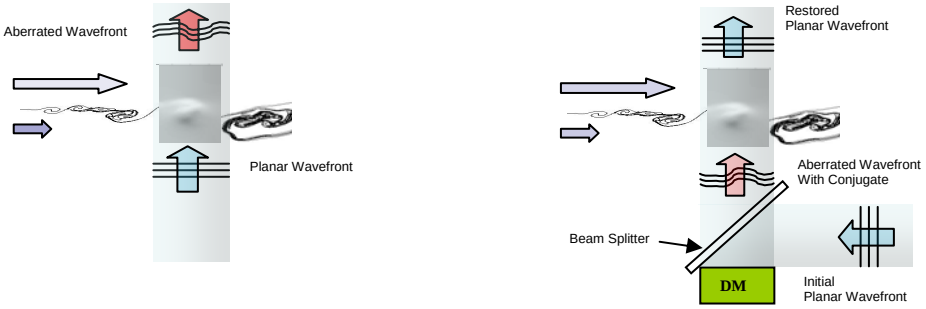

Figure 1. Laser Propagation through an Aberrating Shear Layer. Left: Planar Wavefront Aberrated by the Shear Flow; Right: Effect of Placing an Initial Conjugate Aberration on the Beam Prior to Propagation.

What is often overlooked is that all of these components are part of a complete system driven by a *control loop*. In the traditional approach the control system is a feedback system which forms another bandwidth-limiting step/component in the AO system. This last step has been extensively studied by Tyson[3] and others. In the end it appears that only ~ $1/10^{th}$ of the residual error can be removed for each DM update (usually the clock time of the WFS) in order to keep feedback approaches stable. On the other side of the equation is the *bandwidth requirement*, which is set by the aberrating flow field itself. As described in Tyson[3] and reexamined and affirmed specifically for aero-optic disturbances in Cicchiello and Jumper[4], an aberration must be removed ten times per its aberration-coherence-length clearing time in order to restore 80% of its diffraction-limiting performance. These bandwidth characteristics for an AO system are summarized in Fig. 2 for an aberrating flow that initially reduces the Strehl ratio to less than 0.1. Figure 2 shows that for the traditional adaptive-optic approach, in which an aberration has a clearing frequency through the aperture of 1 kHz, the wavefront sensor must frame at 100 kHz *in real time* in order to restore an 80% Strehl ratio. The fastest real-time wavefront sensors that exist today operate at an order of magnitude lower than this. Even if a real-time wavefront sensor were available, other components in the AO system would form a barrier to correcting a 1 kHz aberration; yet the aberrations posed by a high-Mach subsonic shear layer are at least 1 kHz[5-9].

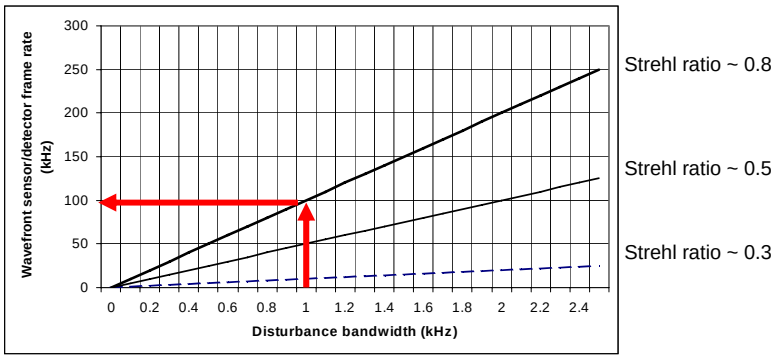

Figure 2. Summary of the Bandwidth Requirements for the Wavefront Sensor given the Bandwidth Requirements imposed by the Aberrating Disturbance and the Limitations of the Control System for the Traditional Approach to Adaptive Optics [Ref. 3].

Realizing that such bandwidth requirements make traditional approaches to adaptive optics unrealistic, we began to explore other possible approaches. In particular, we have proposed an approach that incorporates flow control to "regularize" the shear layer's aberrating character and a feed-forward approach to driving the DM. A companion paper describes a first successful attempt at using this technique

to perform an adaptive-optic correction for propagation through a 240 Hz disturbance due to laser propagation through a two-dimensional, planar heated jet[5]. The success of the heated-jet experiment depended on the fact that shear layers are susceptible to forcing[6]. In the Ref. 5 experiment the planar shear layers forming the jet were acoustically forced and the signal driving the speaker was used to synchronize the waveform driving the DM. This waveform was previously determined from extensive wavefront measurements made for a laser propagating through an acoustically-force heated jet[5]. Although the experiment involved a man in the loop, it demonstrated a number of operations required to optimize both the synchronization and shaping of the waveform to provide the best adaptive-optic correction. In a less contrived application, a control system will be required to perform this optimization without resorting to a man in the loop. In order to develop the required control system it will be necessary to develop models of each component in the system, including the shear layer itself and its optical response to forcing. This paper describes the first steps in performing a system identification of a shear layer's optical response.

In performing this first step, a discrete-vortex-based code was used, which is referred to as the "weakly-compressible model." Developed by Hugo and Jumper[7, 8] and improved by Fitzgerald and Jumper[1], this code was first used to develop wavefront sensors and later to discover the physics of the aberrating mechanism in a matched-total-temperature shear layer[1]. The weakly-compressible model has been shown to closely match the optical response of an unforced shear layer[9, 10]. In this paper we examine the codes predictions of the shear layer's response to forcing. The paper will give a brief description of the code and a review of comparisons between the code's unforced characteristics and those of experimental shear layers. Following this, we will explore the relationship between the shear layer's optical response to forcing and other measures of experimental fluid-mechanic responses to forcing found in the literature. In particular, this paper establishes the relationship between a shear layer's optical response and more-traditional measures of a shear layers character.

II. The Weakly-Compressible Model

A detailed description of the weakly-compressible model, discrete-vortex-based code, can be found elsewhere[1]; however, a brief description of its underlying components will be given here. The code is based on the use of a two-dimensional discrete vortex method to first compute the velocity field for a free shear layer that originates at a splitter plate. The code has been used to simulate the velocity field for shear layers with high-speed sides as high as Mach 1.0. In even the highest-speed cases, the convective Mach numbers are less than 0.45, and as discussed in Fitzgerald and Jumper[1], such shear layers are referred to as weakly compressible, making incompressible approaches to predicting the velocity field only slightly in error when neglecting the dilation terms[1, 11]. The unsteady velocity field resulting from the discrete-vortex method forms the basis for computing the thermodynamic properties. The thermodynamic properties are found by overlaying the momentum and energy equations along with the second law onto the velocity field by first back solving for an initial estimate of the pressure field and then iteratively correcting for the temperature and density fields until a self-consistent field of thermodynamic properties is converged upon. Once the converged density field is known at each time step, the density is converted to index-of-refraction through the Gladstone-Dale constant.

As described in Ref. 1, the largest contributor to the optical aberrations in the shear layer is the formation of coherent structures in the shear layer under the influence of the Kelvin-Helmholtz instability. In the convecting frame, these coherent structures form vortices whose diameters roughly match the vorticity thickness of the shear layer and contain high flow curvature. This curvature gives rise to concomitant pressure gradients that we have shown in turn give rise to relatively deep low-pressure cells or wells within the vortices. These wells are accompanied by drops in the density. Also contributing to the aberrating character of the shear layer are local higher-pressure and density regions that form in the local stagnation regions in the convecting frame. These form at the velocity saddle points along the breads between the vortices (rollers). The most controversial part of this explanation for the physics of the shear layer's aberrating character was the notion that relatively-deep pressure wells could form in a shear layer, since the prevailing thought at the time was that static-pressure fluctuations in a shear layer were negligible, based on the so-called strong Reynolds analogy[1]. However, experiments performed at Notre Dame showed that the actual pressure wells measured in these vortices closely matched the predictions of the weakly-compressible model[8]. The optical character was also shown to closely match the predictions of the weakly-compressible model[9]. Figure 3 gives selected results from these comparisons.

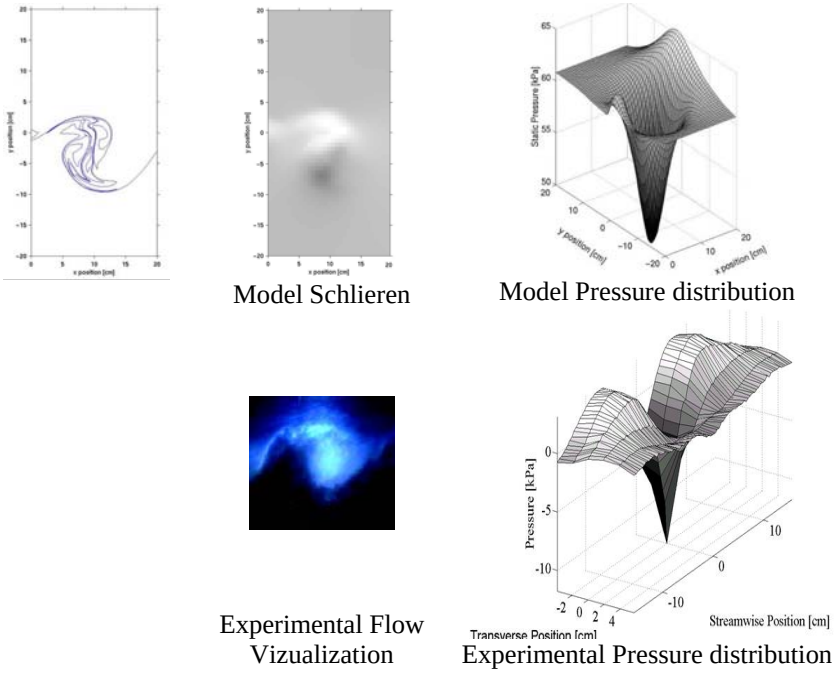

Figure 3. Comparisons between the predictions of the Weakly-Compressible Model[1] (upper figures) and Experiment[8, 9] (lower figures).

Extensive comparisons of the discrete-vortex code with experiments have been reported elsewhere. Among these is the comparison of the amplification of disturbances input at the splitter plate to the theoretical linear-stability amplification factors[12]. These latter comparisons showed good agreement to theory, which itself has been shown to be in good agreement with experiment[12]. Other than these comparisons, no extensive investigation has been performed for general cases of forcing. The next section describes our recent examination of the weakly-compressible model's response to forcing.

III. Response of the Weakly-Compressible Model to Forcing

A recent numerical study by Freund, et. al. showed that the most effective forcing of a shear layer is to displace the edge of the splitter plate in the direction, y, normal to its surface[13]. In the case of the discrete-vortex code, forcing was simulated by inserting the first vortex into the shear layer displaced from the splitter-plate edge in the vertical, y, direction by d

$$d(t) = A\sin\left(2\pi f_1 t + \phi_1\right) + B\sin\left(2\pi f_2 t\right) + \ldots. \qquad (1)$$

where more than one frequency can be forced at different amplitudes, **A**, **B**, etc. and phase shifted by ϕ. In general, most experimental shear layer studies report their results in terms of measures of the shear layer's thickness, the most common of which are either the shear layer's vorticity thickness, δ_ω, or the shear layer's momentum thickness, θ, given respectively by

$$\delta_\omega = \frac{\mathbf{u}_\mathbf{U} - \mathbf{u}_\mathbf{L}}{\left(\dfrac{\mathbf{du}}{\mathbf{dy}}\right)_{\max}} \qquad (2)$$

and

$$\theta = \int_{-\infty}^{+\infty} \frac{\mathbf{u(y) - u_L}}{\mathbf{u_U - u_L}} \left(1 - \frac{\mathbf{u(y) - u_L}}{\mathbf{u_U - u_L}}\right) \mathbf{dy} \tag{3}$$

where u_U and u_L are the upper and lower stream velocities, respectively.

The first comparison is similar to that reported earlier[1]; Fig. 4 shows the growth of the unforced shear layer in terms of its vorticity thickness vs. distance from the splitter plate. These results are for u_U = 261.04 m/s, u_L = 34.7 m/s at the various initial half shear layer thicknesses, $\delta_i/2$, of 8.63 mm, 17.25 mm and 34.5 mm. Extensive experimental results for growth rate of shear layers with convective Mach numbers less than ~ 0.45 was shown by Brown and Roshco[14] to be able to be predicted by

$$\frac{\delta_\omega}{\mathbf{x}} = \mathbf{C}_\delta \frac{(1-\mathbf{R})\left(1+\mathbf{s}^{\frac{1}{2}}\right)}{\left(1+\mathbf{R}\,\mathbf{s}^{\frac{1}{2}}\right)} \tag{4}$$

where $R = u_L/u_U$, $s = \rho_L/\rho_U$, and $C_\delta = 0.085$. For the conditions tested using the code, the growth rate $d\delta_\omega/dx$ was 0.139, while Eq. (4) would predict 0.13[1]; thus, the code predicts a growth rate within 6.5% of those experimental results as reported in Ref. 14. For the remaining results in this paper, $\delta_i/2$ was set equal to 17.25 mm. The results from Fig. 4 can be recast in terms of the momentum thickness.

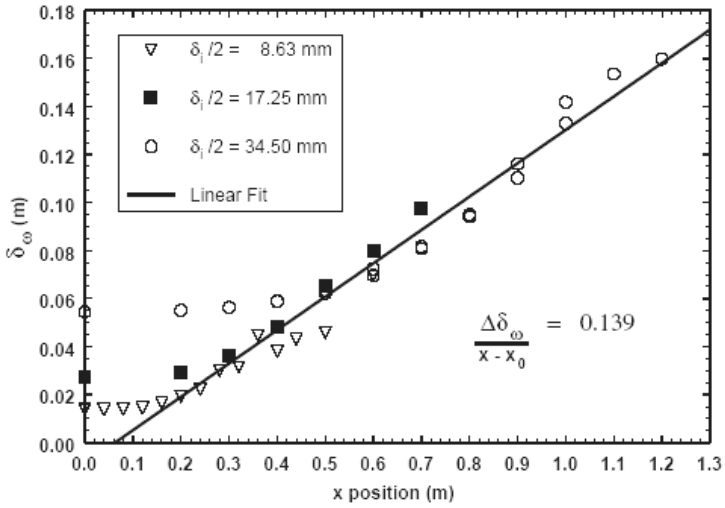

Figure 4. Vorticity thickness versus Distance from the splitter plate for an unforced shear layer.

Single-Frequency Forcing Results. The previous section demonstrates that the code does a reasonably good job at predicting the growth of the unforced shear layer. This section examines the codes response to single-frequency forcing. In addition to showing the unforced shear layer's character, Figs. 5 give the effect of forcing the shear layer at different amplitudes, A, for a fixed frequency, f_1, of 650 Hz as per Eq. (1) [left] and the effect of forcing the shear layer with a fixed amplitude, A, of 2.5 mm and different frequencies [right].

It is clear from Fig. 5 that the effect of forcing the shear layer is to abruptly increase the shear layers thickness and then "stabilize" its growth in thickness for a region that precedes the position where the shear layer would have been at that thickness in the unforced case. The amplitude of the forcing affects the location where the shear layer abruptly rises. Although for different flow conditions, this behavior is very similar to the experimental response reported by Oster and Wygnanski[15]; Figs. 6 give the experimental shear layer response to single-frequency forcing reported in Ref. 15.

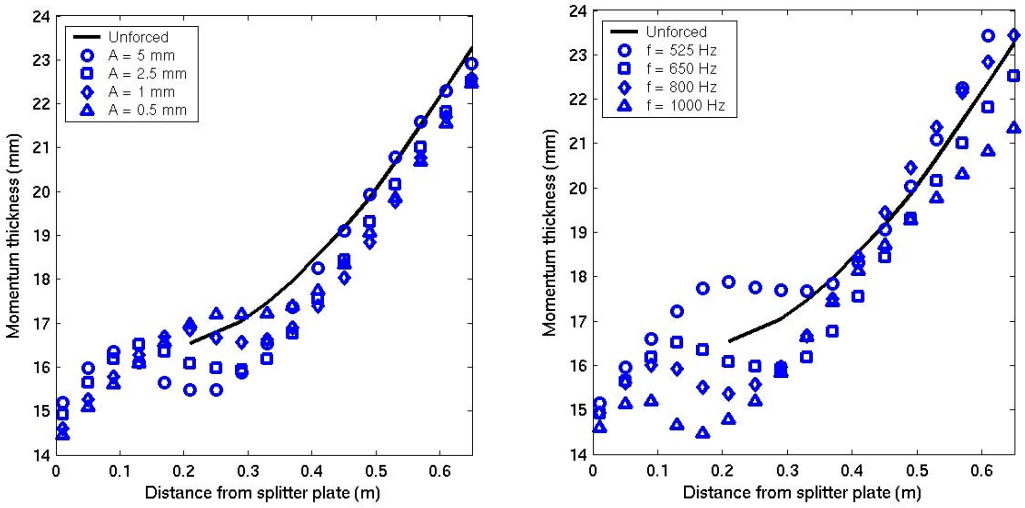

Figure 5. WCM predictions of momentum thickness versus distance for the unforced shear layer and for forcing at 650 Hz and amplitudes of 0.5, 1.0, 2.5 and 5 mm (left) and momentum thickness versus distance for the unforced shear layer and for forcing with a fixed amplitude of 2.5 mm, for frequencies of 525, 650, 800 and 1000 Hz (right).

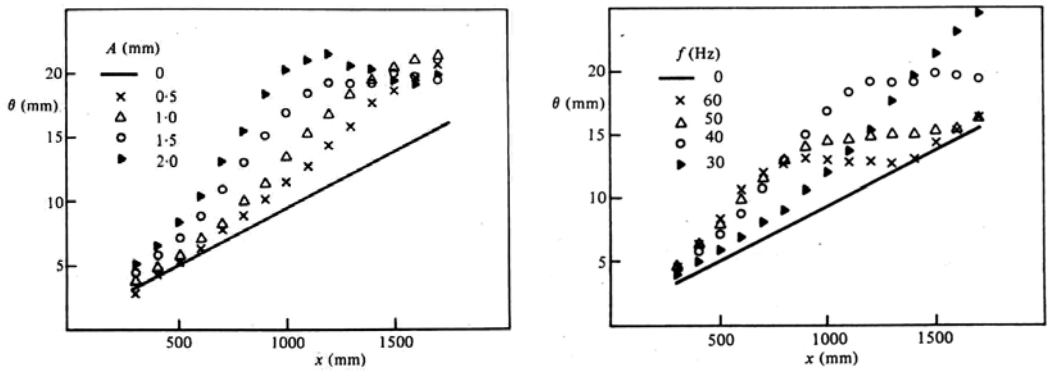

Figure 6. Left: Effect of Amplitude of oscillation of a trailing-edge flap, 1.0 cm long, located at the trailing edge of the splitter plate, forced at 40 Hz on the shear-layer momentum thickness, θ; Right: Effect of frequency of oscillation of a trailing-edge flap, 1.0 cm long, located at the trailing edge of the splitter plate, forced at an amplitude of 1.5 mm on the shear-layer momentum thickness, θ (From Ref. 15).

In a later paper, de Zhou and Wygnanski[16] were able to perform hot-wire measurements of the forced shear layer to observe more closely the detailed forcing effect on the shear layer that gave rise to the flattening of its momentum thickness. A selected result from that paper is shown in Fig. 7, for the phase-lock averaged vorticity field of the shear layer under single-frequency forcing. At least on average, Fig. 7 shows that the shear layer's stabilization in growth is the result of "regularizing" the coherent structures in the shear layer. Similar instantaneous realizations of vorticity were computed from the code results for a shear layer forced at various frequencies.

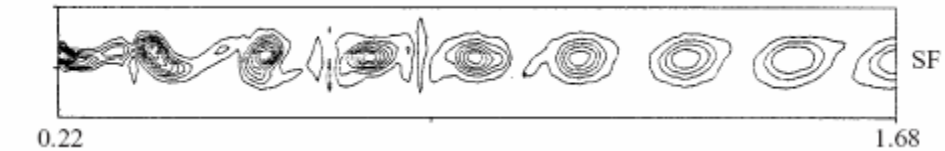

Figure 7. Phase-Lock Averaged Vorticity plot (From Ref. 16).

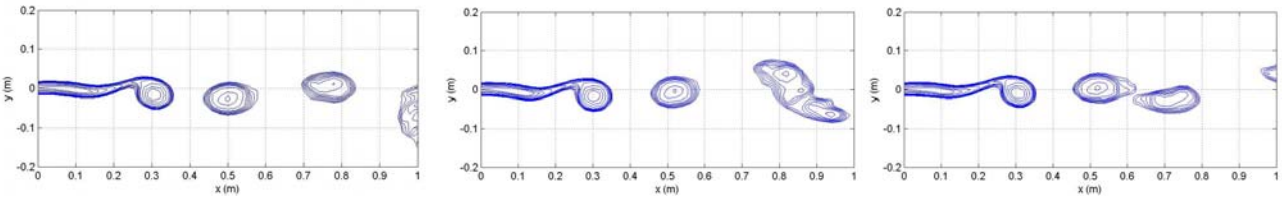

Figure 8. Single Realizations of Vorticity plots for the code forced at 650 Hz, captured at the same phase angles of three successive cycles.

Figures 8 give three realizations of vorticity plots for the shear layer being forced at f=650 Hz with an amplitude of A=2.5 mm, B=0 in Eq. (1) at equal time delays corresponding to the same phase angle of the forcing. The fixed-phase-angle vorticity plots were averaged to produce the results presented in Fig. 9. A comparison of Fig. 9 with Fig. 7 shows that on average, as in the Ref. 16 experiment, the shear layer has been regularized by single frequency forcing; however, phase-lock averaging can be deceptive. As shown in Fig. 9, the decreasing vorticity contours in the downstream region of the shear layer, also present in the experimental plots in Fig. 7, are not an indication of preserving a single vortex, but rather the fact that single forcing controls only the roll up for which the forcing frequency is tailored and the normal process of pairing and merging (see below) continues to progress under the influence of the Kelvin-Helmholtz instability (see Fig. 8). What is clear, however, is that the first roll-up location is "locked" by the forcing and the coherent structure that is formed remains in tact for some distance before being influenced by the uncontrolled merging of vortices.

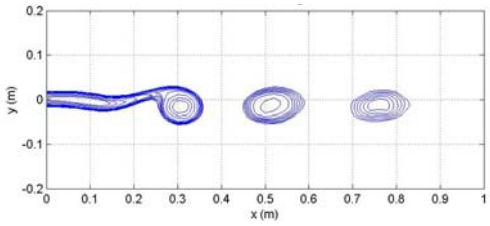

Figure 9. Phase-Lock-Averaged Vorticity plot for the code forced at 650 Hz for the same phase angle given in Fig.8.

Another way of studying the code results is to look at the locus of points indicating the locations of the discrete vortices that define the undulation of the shear layers "contact surface." Figure 10 shows two such "shear- layer loci"; the one on the left is for the unforced shear layer and the one on the right is for the shear layer forced at 650 Hz at an amplitude of 2.5 mm. Figure 11 shows a smaller region of the unforced shear layer (left) and the forced shear layer at 650 Hz (right) at the same phase angle for six cycles. The plots display the region of the furthest extent where the shear layer shows reasonably good control. Taken together, Figs. 9, 10 (Right), and 11 show that the shear layer is extremely well controlled up to the first roll up, and relatively well controlled up to the point where the first vortices begin to merge (second roll up), implying that the single-frequency forcing regularizes the shear layer out to approximately 0.5 m with some marginally-well controlled behavior slightly beyond 0.6 m. This is consistent with the point where the momentum thickness begins to grow again in Fig. 5. Figure 11 (right) shows that the differences from one frame to the next are caused by the encroachment of the "vortex-merging" phenomenon. As arranged, an interesting effect can be noted, which has not been reported elsewhere to our knowledge, that for single forcing near the most-amplified frequency, every third cycle is strikingly similar. Ho and Huang[17] have reported merging of three vortices under the influence of a single–frequency forcing; however, in their case the frequency was much lower than the most-unstable frequency (~ 1/3rd the most-unstable). This similarity prompted us to create phase-lock averaging of the vorticity plots for every third cycle. These are shown in Fig. 12. Figure 12 indicates that a three-cycle repeat at 1/3rd the forcing frequency does a better job of capturing what is actually happening, as can be seen by comparing the phase-lock averaged vorticity plots to the three individual realizations at the same phase angle shown in Fig. 8. Initially we could not understand this phenomenon since the conventional wisdom is that shear layers, on average, increase in size only by pairing and creating subharmonics (i.e., divisions by 2) rather than thirds of a frequency; however, long time series of shear-layer loci showed that once a pairing of the initial-roll-up vortices occurred it would initiate a process that led to the three-cycle repeat. Under the influence of a

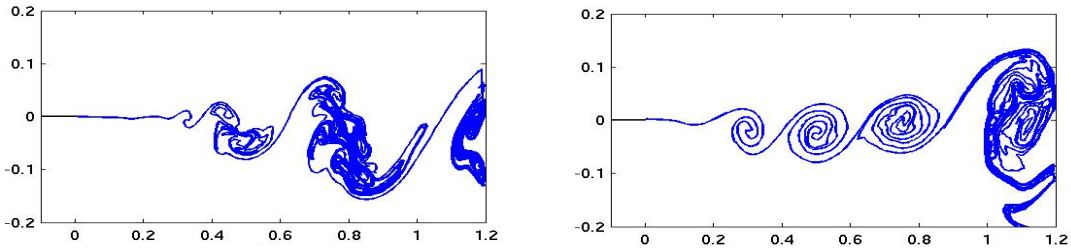

Figure 10. Single Realization of the Shear-Layer Loci for the Unforced (left) and Forced (right) shear layer from the Code, where the shear layer is forced at 650 Hz.

single forcing frequency, the regularized spacing of the first roll up allowed the greater vorticity accumulation (circulation) contained in the larger, paired vortex to create a single structure which merged into a three-initial-vortex agglomerated vortex. This is followed by the next two initial-roll-up vortices undergoing pairing and then the process repeats. This third-vortex merging is shown in Fig. 13, showing equally-time-spaced realizations for one full cycle of this process.

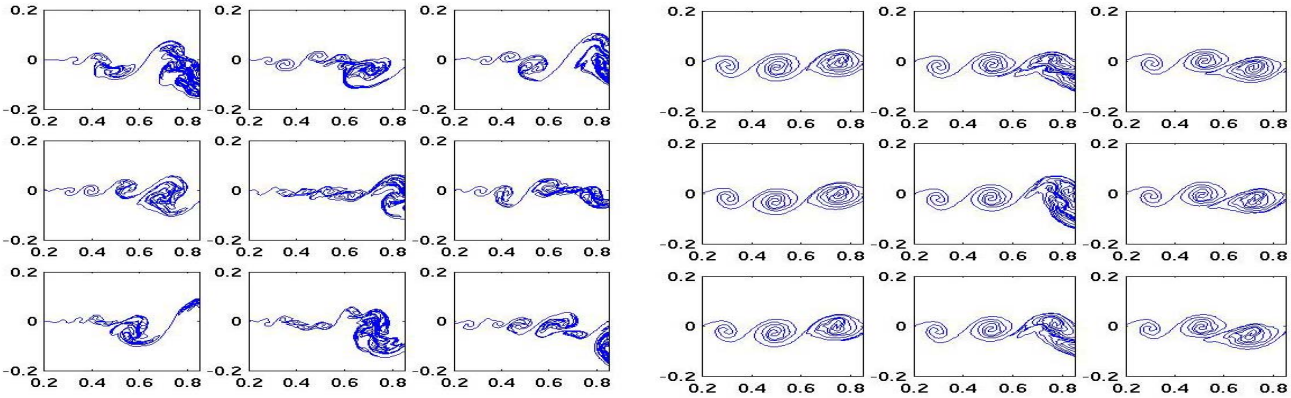

Figure 11. Six successive cycles of Shear-Layer Loci for the unforced (Left) and forced (Right) shear layer from the Code, for a forcing at 650 Hz.

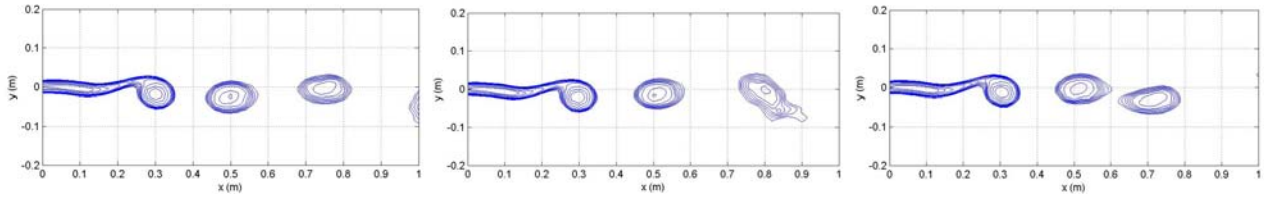

Figure 12. Three Phase-Locke-Averaged Vorticity Plots at the same phase angles as shown as single realizations in Fig. 8, for every third cycle of forcing at 650 Hz.

Two-Frequency Forcing Results. On a statistical basis (as in Fig. 9) forcing at a single frequency appears to produce robust control of the shear layer's first roll up or vortex formation; however, for the purposes of accurately regularizing the shear layer in order to reproduce a near-exact optical aberration cycle after cycle, examination of instantaneous realizations (as in Fig. 11) showed variations on a three cycle repeat. Indeed, a three-cycle repeat did a better job of capturing a more accurately-regularized pattern. But even on a three-cycle repeat the regularization persisted only up to the point where the shear layer matched the unforced thickness after which pairing of the vortices caused the shear layer to begin growing again. This can be seen in the momentum thickness results obtained from the weakly-compressible model (Figs. 5) and from experiment (Fig. 6)[13]. De Zhou and Wygnanski[14] found that adding forcing at the subharmonic can exert some control on the paring. Gordeyev and Thomas[18] similarly found that forcing at the subharmonic can affect the pairing for a planar jet; further more, they found that the

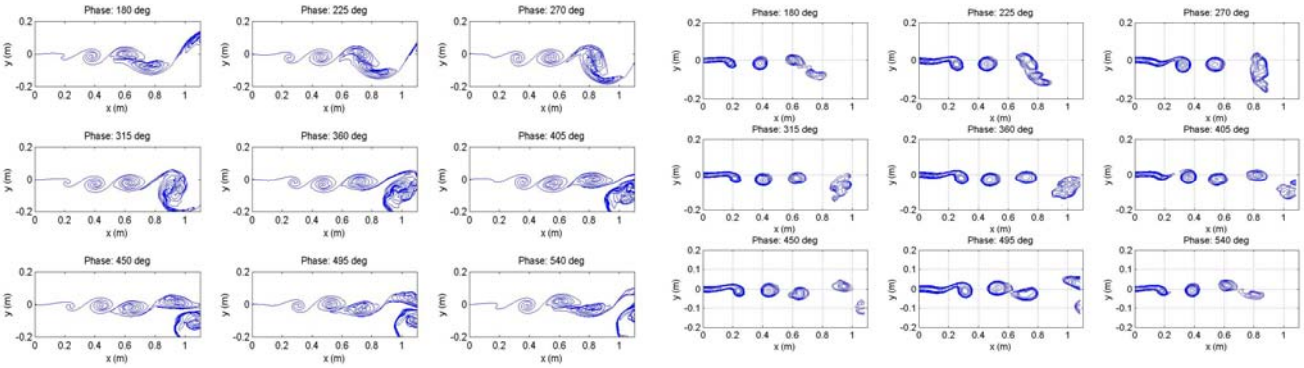

Figure 13. Equally-Time-Spaced Realizations of the Three-Vortex Merging Process: Shear-Layer Loci (Left), Vorticity Plots (Right).

ability to control the pairing was sensitive to the phase angle of the fundamental with respect to the subharmonic forcing frequency. Using the addition of the second term in Eq. (1), subharmonic forcing was explored and we were able to further regularize the shear layer, effectively controlling the location of pairing. As in the case of Gordeyev and Thomas[18], the effectiveness in controlling the subharmonic was sensitive to the phase delay of the subharmonic. Figure 14 shows a series of realizations of the shear layer loci at a fixed phase angle for every cycle of the fundamental forcing frequency on the left and every other cycle on the right, where A=2.5 mm, B=2.5 mm, ϕ_1=320 degrees, and $f_2=f_1/2$=325 Hz in Eq. (1). Two-frequency, fundamental/subharmonic forcing clearly controls the location of pairing and fixes the periodicity to the subharmonic.

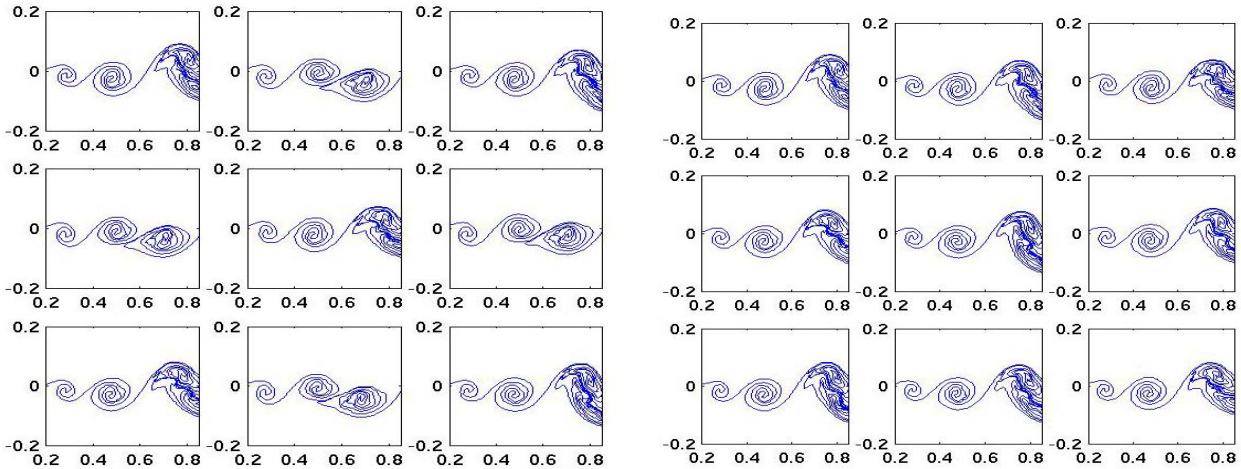

Figure 14. Six Successive-Cycle Realizations of the Shear Layer Loci at the same Phase Angle (Left) and Every Other Cycle (Right).

IV. Optical Response of the Shear Layer

Once the density fields are available as a function of time from the weakly-compressible model, the effect of a laser propagated through the shear layer can be computed. As described in Ref. 1, the index-of-refraction fields are sufficiently weak that a simple integration through the field in the y-direction can be used to compute the optical path length as a function of position and time, OPL(x,t)

$$\mathbf{OPL(x,t)} = \int_{y_1}^{y_2} \mathbf{n(x,y,t)dy} \qquad (5)$$

where the index of refraction, n, is related to the density, ρ, by

$$\mathbf{n(x,y,t)} = 1 + \mathbf{K_{GD}}\rho\mathbf{(x,y,t)} \tag{6}$$

where K_{GD} is the Gladstone-Dale constant. Once the OPL(x,t) is known at an instant in time, the optical path difference over an aperture, A, can be computed by removing the average OPL over the aperture, $\overline{\mathbf{OPL}}\mathbf{(A,t)}$, from the local OPL

$$\mathbf{OPD_A(x,t)} = \mathbf{OPL(x,t)} - \overline{\mathbf{OPL}}\mathbf{(A,t)} \tag{7}$$

A laser's wavefront is a locus of points along which the beam's phase is constant. At a location y_2, as in Eq. (5), the wavefront will be advanced or retarded, as a function of x, from the mean phase over the aperture. It can be shown[19] that the displacement of the wavefront from the mean at an instant in time, t, has the conjugate value of the OPD(x,t). Due to this, it is common for the wavefront to be described as OPD. According to Huygens' Principle, a wavefront will propagate in a direction normal to itself and concomitantly, if a small-aperture laser beam initially normal to an incoming laser's wavefront is directed through an aberrating flow field in the y direction, it will emerge at an angle, θ(x,t), normal to the emerged, aberrated wavefront[7], so that

$$\theta\mathbf{(x,t)} = \arctan\left(-\frac{\mathbf{d\,OPD(x,t)}}{\mathbf{dx}}\right) \tag{8}$$

When a small-aperture beam is projected through an experimental aberrating turbulent flow field, its emerging angle, θ(x,t), can be recorded at high rates (100+ kHz) and the time series of angles is referred to as the beams "jitter." The following results were obtained by numerically propagating small aperture laser beams through the flow field. Time-varying jitter signals were obtained from the weakly-compressible code by calculating OPDs from the density field using Eqs. (5)-(7) and computing jitter angles using Eq. (8).

Jitter Characteristics. In the present paper, we will examine only the jitter signal as a measure of the code-predicted, shear-layer optical response. To begin with, Figs. 15 show the normalized jitter response at a location 0.415 m from the splitter plate, without and with forcing at 650 Hz. The dotted line in Fig. 15 (right) represents a 650 Hz sinusoidal wave phase locked to the numerical jitter signal. It is clear that the jitter has been regularized by forcing producing a waveform of the same frequency as the forcing frequency.

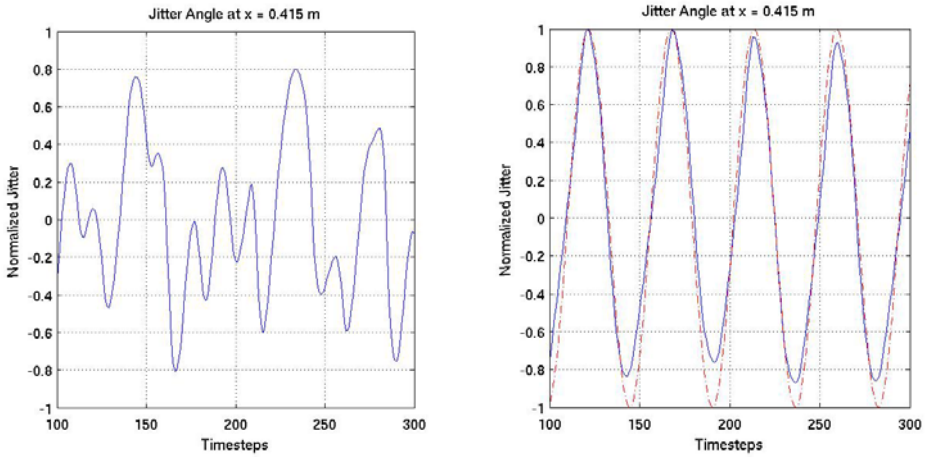

Figure 15. Normalized Jitter versus time computed numerically at a distance of 0.415 m from the splitter plate. Left: unforced and Right: Forced, —— numerically computed jitter, ---- 650 Hz sinusoidal wave.

The frequency content of the jitter signal is clearly related to the coherent structures in the shear layer[1], and as such contains information about the coherence lengths of the aberrating structures convecting through the beam. Figure 16 gives the power spectral density, PSD, of the jitter signal at selected locations from the splitter plate. A mean or "natural optical frequency" at each x-location was computed from the PSD's,

$$f_n(x) = \frac{\int PSD(f,x)\ f\ df}{\int PSD(f,x)\ df} \tag{9}$$

where the n subscript on f indicates the "natural," unforced *optical* frequency in the shear layer at the particular x-location. Figure 17 gives plots of the natural optical frequency, f_n, versus distance from the splitter plate.

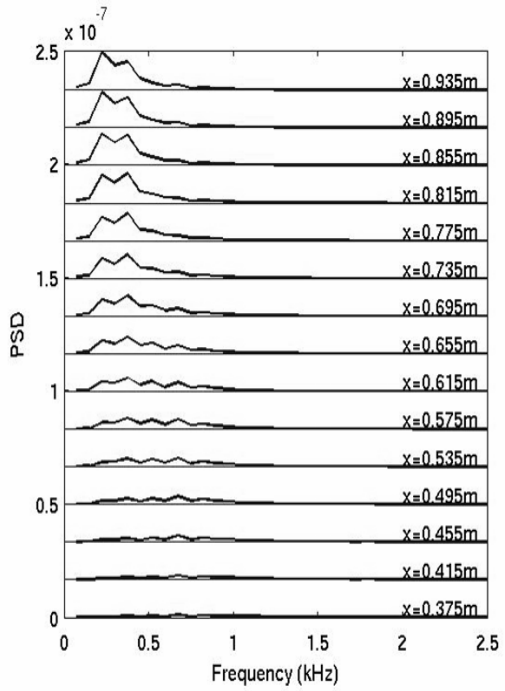

Figure 16. PSD for flow-induced jitter angles at various locations away from the splitter plate.

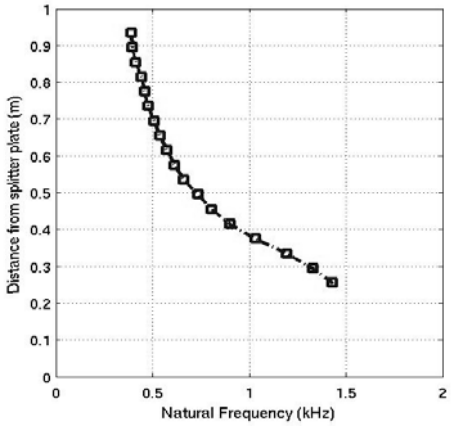

Figure 17. Natural optical frequency, f_n versus Distance from the Splitter Plate for the Unforced Shear Layer.

As mentioned above, these frequencies can be related to an average *optical* coherence length by dividing the convection velocity by the frequency as

$$\Lambda_n(\mathbf{x}) = \frac{\mathbf{U}_c}{\mathbf{f}_n(\mathbf{x})} \tag{9}$$

Figure 18 shows a plot of the natural optical coherence length versus distance from the splitter plate.

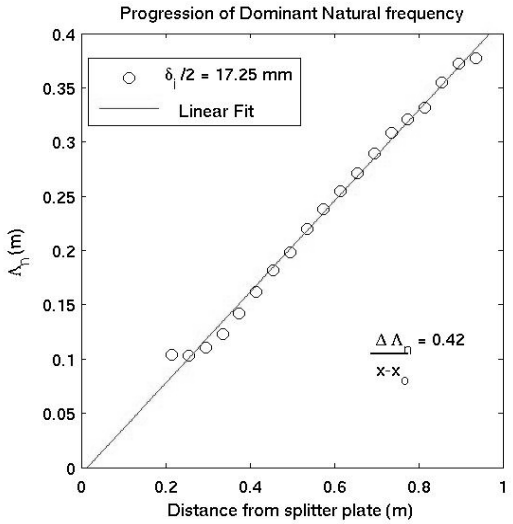

Figure 18. Natural Coherence length in meters versus distance away from the splitter plate.

It is well known that a shear layer's growth is related to the ever-increasing size of the coherent structures that form through pairing and merging. A comparison between Figs. 4 and 18 shows that the relationship between the growth of the optical coherence length in the x direction and the growth of the shear layer thickness is approximately 3. It is important to notice that this factor of 3 is larger than the factor of 1.5 – 2.0 for the relationship between coherent-structure scale size in a shear layer and δ_{vis}[20]; however this difference is attributable to our definition of the natural optical frequency in Eq. (9). Equation 9 is weighted toward the larger structures because the optical response increases approximately linearly with the size of the structure. Since the vorticity thickness is a close measure of the actual thickness of the shear layer, and the optical coherence length closely defines this thickness, the factor of 3 being the relationship between the coherence length in the x direction (related to vortex spacing) and the coherence length in the y direction (vortex size).

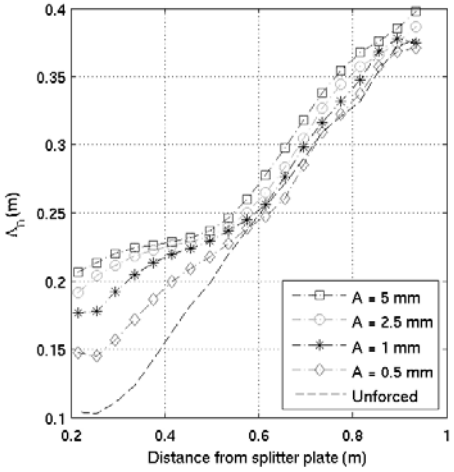

Figure 19. Optical coherence length versus distance for the optical response of a shear layer forced at 650 Hz for varying forcing amplitudes.

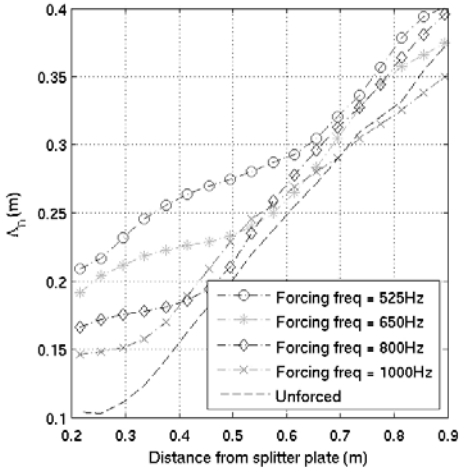

Figure 20. Optical coherence length versus distance for the optical response of a shear layer forced at various frequencies, at an amplitude of 2.5 mm.

Similar plots of optical coherence length versus distance from the splitter plate can be computed under the influence of forcing. Figure 19 shows the effect of forcing the shear layer at a single frequency, 650 Hz, while varying the forcing amplitudes, A, as per Eq. (1). It is clear that the information contained in Fig. 19 and Fig. 5 display a similar trend. The obvious difference in the two figures is that the momentum

thickness shows a flatter slope in the "region of regularization" than the optical coherence length. Examination of the shear layer loci, as in Fig. 10 (right), shows that as the regularized structures evolve and convect, the spacing between them grows slightly in the flow direction while retaining approximately the same thickness in the y direction, thus causing the frequencies to decrease slightly with distance in the regularized region. The shear layer's spreading rate is therefore slightly suspended before pairing and continuing to spread again. The obvious effect of increasing amplitude is to move the sudden thickening of the shear layer, related to the structure roll-up, closer to the splitter plate. This is in agreement with what is known from conventional approaches which measure the growth of shear layers under the influence of forcing[6,13].

Figure 20 displays the effect of varying forcing frequencies with a fixed forcing amplitude of 2.5 mm. Like Figs. 5 (Right) and 6 (Right), Fig. 20 shows that reducing the forcing frequency moves the abrupt increase in optical coherence length further down stream, causing the shear layer thickness to increase with decreasing frequency at locations within the controlled region. This numerical study has not only demonstrated that it is possible to optically regularize a high-velocity shear layer, but also has provided insight into the repeat pattern that can be expected under one- and two-frequency forcing. It should also be noted that forcing the shear layer regularizes the optical response upstream from the location at which the unforced natural frequency would have appeared.

These results demonstrate that optical interrogation of a variable-index-of-refraction shear layer (due in this case to "compressibility" effects) yields similar information to other methods of documenting the shear-layer's characteristics. Because a linear relationship exists between the shear layer thickness, δ_{vis}, and its optical coherence length, Λ_n, optical measurements provide a non-intrusive means of measuring the shear layer's local thickness and could be useful when intrusive ways of measuring thickness are difficult or impossible, as in chemically- or thermally-hostile environments (jet-engine exhaust, for example). Such optical characterization can be as simple as propagating small-aperture lasers through the shear layer, as is in common use in aero-optical investigations at Notre Dame.

V. Conclusions

Numerical two-dimensional high-Mach-number shear layers and related optical aberrations were studied using a discrete vortex method coupled with the Weakly-Compressible Model. These studies showed that the model qualitatively and quantitatively matched experimentally-observed shear layer evolution, including the correct growth rate. One- and two-frequency forcing of the shear layer at the splitter plate location were investigated. The single-frequency-forcing results qualitatively matched experimentally-observed results for lower-velocity shear layers. In comparison to the unforced, naturally-developed shear layer, single-frequency forcing stabilized the vortex roll-up location along with the approximate location of the first pairing/merging. Previously unreported three-vortex merging event was observed in the numerical shear layer simulation, when two subsequent vortices undergo a pairing event and then absorb the following single vortex. Two-frequency forcing with a proper phase shift was also tested and vortex pairing was further stabilized compared with the one-frequency forcing case, robustly controlling the first pairing. Stabilizing the pairing resulted in a precise event repeat at the subharmonic. Stabilizing the fluid mechanics of the shear layer also regularized the optical characteristics of the shear layer. This was shown by computing the time-varying OPD(t,x) imposed on a collimated laser beam passing through the shear layer as a function of time and downstream distance. In the forced and unforced cases, streamwise optical coherence lengths were calculated from OPD spectra and were shown to provide essentially the same information as the momentum or the vorticity thicknesses regarding the shear layer's growth rate. Since OPD measurements are done non-intrusively, information about the strength and growth rate of any variable-index-of-refraction shear layer can be extracted from optical measurements, without using intrusive velocity sensors like hot-wires or Pitot probes.

Recall that this study was performed specifically to investigate the applicability of the numerical model in constructing a low-order "transfer function" for use in obtaining a shear-layer system identification functional representation for use in investigating feed-forward control systems. Preliminary results, like those in Fig. 15, indicate that such a low-order representation is feasible and future papers will address such models. But these results have provided some unexpected new insight into anomalies that have been observed in on-going adaptive-optic studies at Notre Dame. As reported in Ref. 5, although a heated jet used in that work was being forced at 240 Hz, the optical pattern was observed to repeat at its subharmonic. It is clear from the present study that this subharmonic repeat is due to the paring event

which is only approximately controlled by single-frequency forcing. The fact that the pairing was only approximately controlled has been shown to be the largest source of inaccuracies in the adaptive-optic corrections. In future experiments, two-frequency forcing will be used in an attempt to further improve the already spectacular results reported in Ref. 5. Further, in a separate experimental investigation at Notre Dame, a Mach 0.85 shear layer is being forced in an attempt to regularize its optical response. Results from the numerical study have been instructive in guiding the approach to forcing, which is markedly different from approaches that had been tried prior to this numerical investigation.

Acknowledgments

These efforts were sponsored by the Air Force Office of Scientific Research, Air Force Material Command, USAF, under Grant Number F49620-03-1-0019. The U.S. Government is authorized to reproduce and distribute reprints for governmental purposes notwithstanding any copyright notation thereon.

References

[1]Fitzgerald, E.J. and Jumper E.J., "The Optical Distortion Mechanism in a Nearly Incompressible Free Shear Layer," *Journal of Fluid Mechanics*, Vol. 512, 2004, pp. 153-189.

[2] Cicchiello, J.M., Fitzgerald, E.J. and Jumper, E.J., "Far-Field Implications of Laser Transmission Through a Compressible Shear Layer," *Free-Space Laser Communication Technologies XIII Conference*, **4272**, SPIE, San Jose California, 20-26 January 2001, pp. 245-259.

[3]Tyson, R.K., Principles of Adaptive Optics, Academic Press, Inc., San Diego, 1991.

[4]Cicchiello, J.M., and E.J. Jumper, "Far-Field Optical Degradation due to Near-Field Transmission through a Turbulent Heated Jet," *Applied Optics*, **36** (25), pp. 6441-6452, September 1997.

[5]Duffin, D.A., "Feed-Forward Adaptive-Optic Correction of Aero-Optical Aberrations Caused by a Two-Dimensional Heated Jet," AIAA Paper 2005-4776, June 2005.

[6] Ho, C-M, and Huerre, P., "Perturbed Free Shear Layers," *Annual Reviews of Fluid Mechanics*, **16**, 1984, pp. 365-424.

[7]Jumper, E.J., and E.J. Fitzgerald, "Recent Advances in Aero-Optics", *Progress in Aerospace Sciences*, **37**, 2001, pp.299-339.

[8]Jumper, E.J., and Hugo, R.J., "Quantification of Aero-Optical Phase Distortion Using the Small-Aperture Beam Technique," *AIAA Journal*, **33**(11), 1995, pp. 2151-2157.

[9]Chouinard, M. Asghar, A., Kirk, J.F., Siegenthaler, J.P. and Jumper, E.J., "An Experimental Verification of the Weakly-Compressible Model, AIAA Paper 2002-0352, Jan 2002.

[10]Fitzgerald, E.J., Siegenthaler, J.P. and Jumper, E.J., "Optical Characterization of the Notre Dame Compressible Shear-Layer Facility," AIAA Paper 2002-2274, May 2002.

[11]Eldredge, J.D., Colonius, T. and Leonard, A., "A Dilating Vortex Particle Method for Compressible Flow," *Proceedings of the ESAIM, Fourth International Workshop on Vortex Flows and Related Numerical Methods*, 2000.

[12]Hugo, R.J., *Aero Optical Effects*, Dissertation, Notre Dame, 1995.

[13]Freund, J.B. and Wei, M.," Some Small Changes that Make a Mixing Layer Very Quiet", AIAA Paper 2005-0997, Reno, Jan 2005.

[14]Brown, G. L. and Roshko, A., "On density effects and large structure in turbulent mixing Layers," *Journal of Fluid Mechanics* **64**(4), pp. 775-816, 1974.

[15]Oster, D. and Wygnanski, I, "The Forced Mixing Layer between Parallel Streams," *Journal of Fluid Mechanics*, **123**, 1982, pp. 91-130.

[16]de Zhou, M. and Wygnanski, I., "The Response of a Mixing Layer formed between Parallel Streams to a Concomitant Excitation at Two Frequencies," Journal of Fluid Mechanics, 441, pp. 139-168, 2001.

[17]Ho, C.M. and Huang, L-S., "Subharmonics and Vortex Merging in Mixing Layers," *Journal of Fluid Mechanics*, **119**, pp. 443-473, 1982.

[18]Gordeyev S.V. and Thomas F.O., "Temporal Subharmonic Amplitude and Phase Behavior in a Jet Shear Layer: Wavelet Analysis and Hamiltonian Formulation", *Journal of Fluid Mechanics*, vol. **394**, pp. 205-240, 1999.

[19]Klein M.V., *Optics*. New York: Wiley, 1970.

[20]Dimotakis, P.E., "Two-Dimensional Shear Layer Entrainment," *AIAA Journal*, **24** (11), pp. 1791-1796, 1986.